Imperial College London

IMPERIAL COLLEGE LONDON

DEPARTMENT OF MECHANICAL ENGINEERING

LITERATURE REVIEW PROJECT

NANOFUELS FOR THE CONTROL OF ENGINE EMISSIONS

Author: Asad Raja

Supervisor: Andrea Giusti

CID: 01347819

Date: 13/12/19

Word Count: 10542

Page Count: 30

Aims

The aims of this literature review are as follows:

1. To provide an insight into the effects that nanofuels may have on both the local scale and the global scale when used to improve combustion in an engine.
2. To consider the practicality of nanofuel use in terms of their preparation and the limitations of their use.

When considering the effect of nanofuel use, the scope has been limited to a discussion of the combustion chamber interactions and engine performance and emissions. Mathematical modelling of combustion behaviour effects will therefore not be discussed.

Abstract

The use of nanofuels is a novel development in engine fuel research and shows strong potential to optimise engine performance and emission behaviour as well as droplet scale effects. This review considers these behavioural effects and identifies verified trends in the literature, as well as areas for further consideration. The practical implementation of nanofuels has also been outlined with respect to their preparation and limitations to consider such as health and environmental effects.

Contents

1. Introduction

1.1. Why Nanofuels?

The field of nanofuels is becoming an area of increasing intrigue due to mounting environmental, economic and political pressure to reduce combustion emissions and increase process efficiency. Nanofuels are defined as fuels that contain nanoparticles in a base fuel. These nanoparticles are often metals, metal oxides or metalloids, although research has also been conducted into alternatives, for example multi wall carbon nano tubes (1), graphene oxide nanoparticles (2) and biodegradable carbon quantum dot nanoparticles (3). The latter attempts to address the concern of nanoparticles' toxicity and environmental damage when released in emissions, a pertinent issue that will be considered further in Section 5. Similarly, although most research has used diesel as the base fuel, the use of ethanol or biodiesels and its blends has also been considered (4). Nanoparticle addition is hoped to alter a fuel's thermo-physical properties in such a way to achieve the stated goal of emission reduction and efficiency enhancement – the additives allow for increased conductivity, mass diffusivity and radiative heat transfer (5).

The effect of nanofuels have been concluded as generally positive in research, with an apparent pattern of reduction in certain emissions and an increase in the burning rate and hence engine efficiency. The combustion chamber mechanisms through which these effects are achieved include the increasing of evaporation rates through better radiation absorption, increasing of atomisation due to droplet fragmentation and micro explosions, increasing of ignition rates due to a greater surface area to volume ratio and flame disruption, catalysing of oxidation reactions and reactive nanoparticle agglomerate ignition (5). These mechanisms will be considered in detail in Section 3.

Though the potential for an increase in brake thermal efficiency, a decrease in specific fuel consumption and a reduction in certain emissions is seen in all nanoparticle-base fuel combinations tested in research, the specifics of the optimal conditions and emission effects vary significantly, in particular, with regards to NOx emissions. For example, where aluminium-diesel and iron-diesel nanofuels have been found to increase NOx emissions by 5% and 3% respectively at high loads due to increased exhaust temperatures (6), manganese-diesel nanofuels were reported to have reduced NOx emissions by 4% (1). Silver nano particle additives in biodiesel-diesel blends have also been reported to increase NOx emissions significantly – by 25.3% (7). Likewise, where some authors have observed an increase in CO emissions with the use of nanofuels, others have observed a decrease (8). Combustion and emission properties have been

found to depend not only on the specific nanoparticle and base fuel combination, but on the shape, size and concentration of nanoparticles (5).

The use of nanofuels has been shown to reduce ignition delay, cause rapid oxidation and more complete combustion (9). For aluminium, boron and iron nanoparticles in diesel, the ignition delay went down to 0.2 seconds compared to 1.2 seconds for pure diesel (6). This was related to the reduction in peak pressure seen in these nanofuels. The peak pressure was shown to decrease the most for aluminium, down to 55 bar from 62 bar for pure diesel (6), although this is contrasted by the increase in peak pressure to 63 bar observed by Shaafi et al. for the same combination of aluminium and diesel (10). Clearly, there is still some work to be done on identifying concrete trends of combustion behaviour, a base outline of which has been presented in Section 4.

The stability of nanofuels is an area of concern also. Research has therefore been conducted into the use of surfactants in the synthesis of nanofuels to remove surface tensions, enhancing the fuel's shelf-life. The synthesis of nanofuels has been considered in the Section 2.

The literature review concludes with a discussion of the research conducted thus far and open questions that remain.

1.1.1. Nanoparticles vs. Microparticles

Studies comparing the use of nanoparticle additives to microparticle additives have found that the higher specific surface are of nanoparticles allows for greater reactivity and catalytic activity (5). Indeed, below a diameter of 5-10 nm, the ratio of surface area to bulk atom number of particles has been shown to increase rapidly, ~25% for a 5 nm diameter iron crystal increasing to ~90% for 1 nm (11). The decrease in activation energy that this causes is shown by the mass gain of a nano aluminium sample in diesel during the initial oxidation phase being 3.5 times greater than that of micro aluminium (4). The stability of nanoparticles is also seen to be better than that of microparticles; nanoparticles being lighter means that the probability of their sedimentation is lower (12). Their stability has also been seen to increase with dynamic motion (12). A difference in particle size also results in a different particle agglomeration mechanism – where microparticles form densely packed and impermeable droplet shell structures due to their motion being dominated by orthokinetic transport, nanoparticles form porous and more uniformly distributed droplet shells at the same particle loading rates due to their motion being dominated by Brownian diffusion (5). This contributes to the significant microexplosion behaviour that leads to reduced ignition delay in nanofuels, as will be discussed in Section 3.

2. Preparation of Nanofuels

The two-step method is the most popular way to synthesise nanofuels in literature (13). This method involved nanomaterials being produced in the form of dry powders by either chemical or physical methods, before dispersing the powder in a fluid (13) (14). The nanosized powder may be dispersed in the fuel by intensive magnetic forced agitation (13) or by ultrasonic agitation (13) (14) (15) (16) (17). The ultrasonic agitation method works by causing microscopic vacuum bubbles to form and collapse quickly, resulting in localised pressure waves that introduce shear gradients, thereby overcoming van der Waals attractive forces between particles (15). Indeed, the stability of a nanofuel defined as the resistance to particle agglomeration, is determined by the balance of van der Waals to electric double layer repulsive forces between particles as they approach one another under Brownian motion (18).

An alternative to the two-step method is a one-step method that simultaneously produced and disperses nanoparticles within the base fuel (13). An attempt at synthesising a copper additive nanofuel has been made using this method, with the reduction of $CuSO_4 \cdot 5H_2O$ with $NaH_2PO_2 \cdot H_2O$ in ethylene glycol under microwave irradiation (19). Though this one-step method was successful at creating a stable copper nanoparticle suspension, one-step methods are treated with caution since residual reactants are left in the base fuel, making it difficult to discern the effects of these impurities and those of the nanoparticle (13).

There a three common ways of measuring nanofuel stability. One of these is the direct measurement of the sediment weight and volume under an external force (13). Another is the use of the zeta potential, which is the difference between the electrical potential of the dispersed medium and that of the stationary layer of fluid attached to dispersed particles (13). This can be linked to the stability of the nanoparticle suspension. The absorption spectrum of a nanofuel can also be examined to determine the sedimentation kinetics of additives (18). To increase stability, the use of surfactants is necessary in order to increase the contact between the two phases and therefore reduce the likelihood of nanoparticle collision and agglomeration (13). The specific surfactant that should be used depends on the solvent characteristics of the base fuel, as well as the solubility characteristics of the nanoparticles. However, the chemical structure of the surfactant should consist of a hydrophobic tail portion, a long-chain hydrocarbon and a hydrophilic polar head group (13).

Research has shown that the concentration of surfactant effects the combustion chamber phenomena of nanofuels, increasing evaporation rates to an extent beyond which monolayer formation over nanofuel droplets causes a reduction in evaporation rates (20). It has also been found that surfactants' effect on stability is damped at high temperatures (21).

3. Nanofuel Droplet Combustion Chamber Interactions

The classification of nanofuel droplet combustion chamber phases depends on the behaviour of the specific base fuel – additive combination in addition to external parameters. However, evaporation and secondary atomization phases are common to almost all nanofuels, as with pure fuel droplets (22). Deviation from the behaviour of pure fuel droplets can be seen in the specific modes of these phases, as well as the potential catalytic contribution of nanoparticles (1).

3.1. Evaporation Effects

The evaporation rate of fuel droplets influences the fuel's ignition time, which in turn effects the rate of combustion and the completeness of the combustion. This dictates the efficiency of the combustion process and the emission released as a result (22). This section will first look at the classification of the nanofuel droplet evaporation phases, before considering mechanisms by which the presence of nanoparticles enhances evaporation.

3.1.1. Evaporation Phases

As more heat is transferred to pure fuel droplets, their size decreases as fuel is progressively vaporised before the droplet-gas mixture eventually reaches its ignition temperature. Two main phases exist in this process (22). The first is the heat up phase. Here, there is minimal transfer of mass from the droplet, and the concentration of fuel vapour on the liquid surface is low. This is because the majority of heat is used to raise the temperature of the droplet, before part of it begins to be used in feeding the latent heat of vaporisation. As shown in Figure 1, the square of the diameter of the droplet, its size, decreases at a relatively constant rate, though at a much slower rate than the subsequent phase. A point is reached where enough fuel vapour is present on the liquid surface due to accumulation from contribution to the latent heat of vaporisation that there is a decrease in heat transferred to the droplet, making the droplet temperature more uniform.

In the second phase, the steady state, the entire heat gained by the droplet begins to contribute to the latent heat of vaporisation, causing the droplet size to fall at a far greater rate. The size of the heat up and steady state phases depend on the volatility of the droplets and the heating conditions. Godsave has shown that the trend in decrease in droplet size with time in each of these phases can be shown to follow a straight line with gradient equal to a parameter denote the 'evaporation constant' (23). This is known as the D^2 Law (Equation 1).

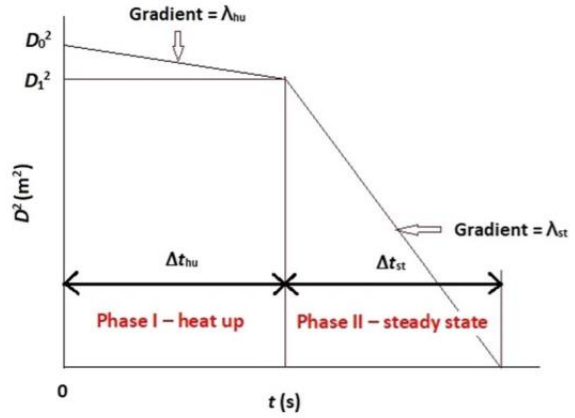

Figure 1: Variation in pure fuel droplet size with time under constant heat addition (4).

$$D_0{}^2 - D^2 = \lambda t \qquad 1$$

For nanofuel droplets, there are three stages of the evaporation mechanism (22). The first two are the heat up and steady state phase as with a pure fuel droplet. The third stage can either be a droplet dry-out phase, or a microexplosion phase. In the dry-out phase, there is near complete evaporation of the base fuel, leaving some residual nanoparticles. In the microexplosion phase, which occurs at temperatures much greater than the boiling point of the base fuel, rapid droplet distortion and disruption occurs. This phenomenon will be explored in greater detail in Section 3.2.

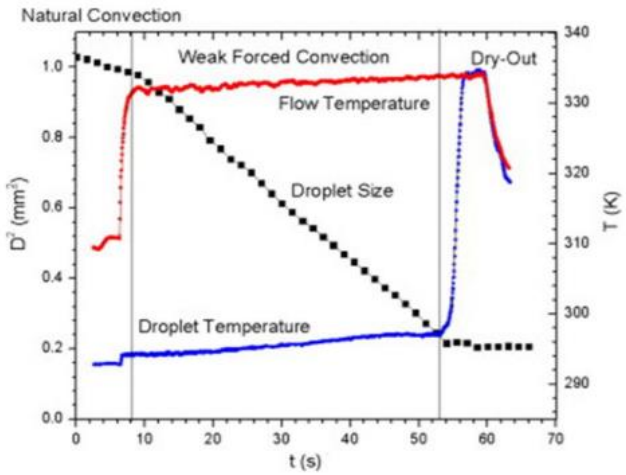

Figure 2: Variation in droplet size with time for an aluminium-ethanol nanofuel (4).

The heat up to steady state to dry out phase behaviour has been observed, for example, in aluminium-ethanol nanofuels (2.5 wt%) undergoing natural and weak forced convection, with nanoparticle agglomerates of about 100 µm being left behind at the end of the dry out phase (24). A graph demonstrating these results is shown in Figure 2. Note that in the dry out phase, the droplet temperature resembles the flow temperature as vaporisation ceases and the nanoparticle agglomerates attain a thermal equilibrium with the flow.

The heat up to steady state to microexplosion phase behaviour has been observed, for example, in aluminium-kerosene nanofuels with an oleic acid surfactant at high temperatures (700 °C and 800 °C) (25). At temperatures below this, a dry out phase behaviour dominates. The increased importance of the microexplosion phase for high temperature values can be shown by the graphical results in Figure 3 that capture the increased volatility and a deviation from the D^2 Law that results at these temperatures due to the droplet deformation and particle expulsion induced (26). The overall evaporation time is made shorter because of these microexplosions. For these high temperatures, some droplet fragmentation is also observed in the heat up phase. This is most likely due to the nanoparticles in the droplets providing some bubble nucleation sites. These generated superheated vapours that may have led to this droplet fragmentation. At the later stages of the evaporation process, most of the fuel droplets would have been evaporated, leaving behind nanoparticle agglomerates. These agglomerates are heated, and in turn heat up the remaining fuel liquid, rupturing the droplets in a series of micro-explosions (26) (20).

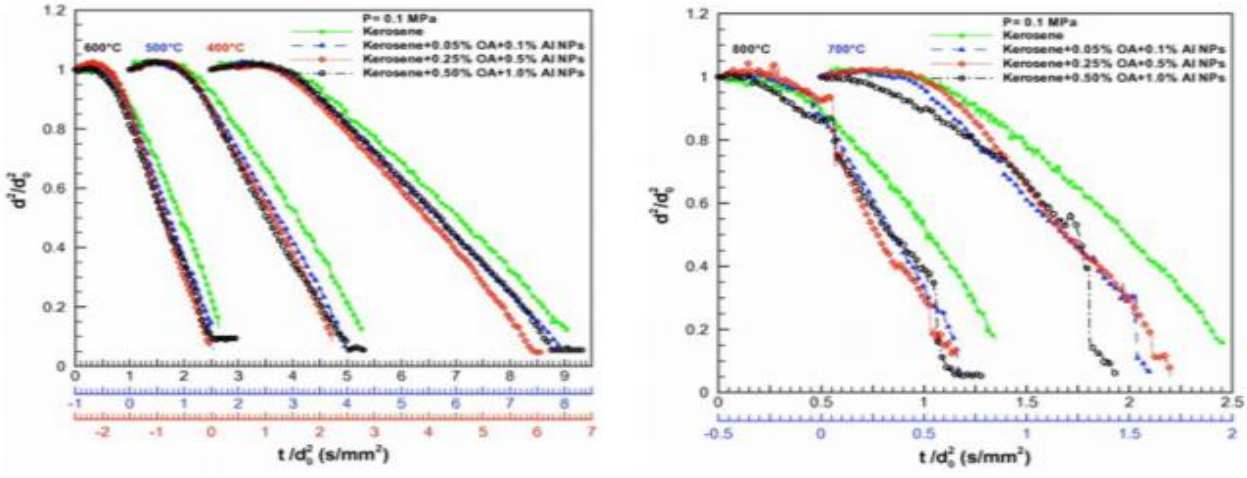

Figure 3: Variation of droplet size with time for aluminium-kerosene nanofuels of varying concentrations at temperatures in the range of 400°C to 800°C (4).

3.1.2. Evaporation Enhancement Mechanisms

There are a few interdependent and simultaneous mechanisms for how nanofuels may increase the evaporation rate. One of these is the radiative absorption and thermal conductivity properties of the nanoparticle causing an increase in droplet temperatures and therefore faster evaporation (22). This effect has been proven significant, the evaporation rate of ethanol with aluminium additives being shown to exceed that of pure ethanol for each of three particle loading rates at any given radiation intensity between 75 W to 175 W (27). This is shown in Figure 4 below. For the optimum particle loading rate of 0.5 wt% aluminium, the evaporation rate was increased by 18% compared to pure ethanol at a radiation intensity of 175 W (27). It was also found that droplet evaporation rates increased nearly linearly with intensity of radiation.

Results for the different aluminium nanoparticle concentrations revealed that increasing the concentration from 0.1 wt% to 0.5 wt% increases the evaporation rate as more radiative absorption takes place (27). However, at a higher concentration of 5 wt%, the evaporation rate is made to decrease (although it is still greater than the rate of evaporation of a droplet of pure ethanol). This is believed to be due to large aggregation of the nanoparticles forming on the surface of the droplet due to an increased frequency of collisions between nanoparticles, which inhibits the diffusion of base fuel to the droplet surface and suppresses evaporation. For aluminium oxide additives in ethanol on the other hand, their far weaker radiative absorption effect means that an increase in concentration from 0.1 wt% to 0.5 wt% does not cause a marked increase in the evaporation rate, and a further increase to 5 wt% actually decreases the evaporation rate compared to pure base fuel as shown in Figure 4 (27). This demonstrates the importance of radiative absorption as an evaporation mechanism, whilst also confirming the existence of a transition temperature for trends in evaporation rate with nanoparticle concentration.

Since the continued evaporation of a nanofuel droplet increases the nanoparticle concentration in the droplet, a transition in the evaporation rate can be observed with time beyond the point at which the transition concentration is reached (21). This behaviour has been observed for nanoparticles of both Fe_2O_3 and Ag in deionized water (21), as well Al in kerosene where the transition concentration was 2.5 wt% Al (28). It has been suggested that increasing the particle loading rate up until the transition concentration also results in greater evaporation rates due to scattering of light caused by the nanoparticles, which increases the length of the radiation's path and may increase the amount of radiation energy that is absorbed (27).

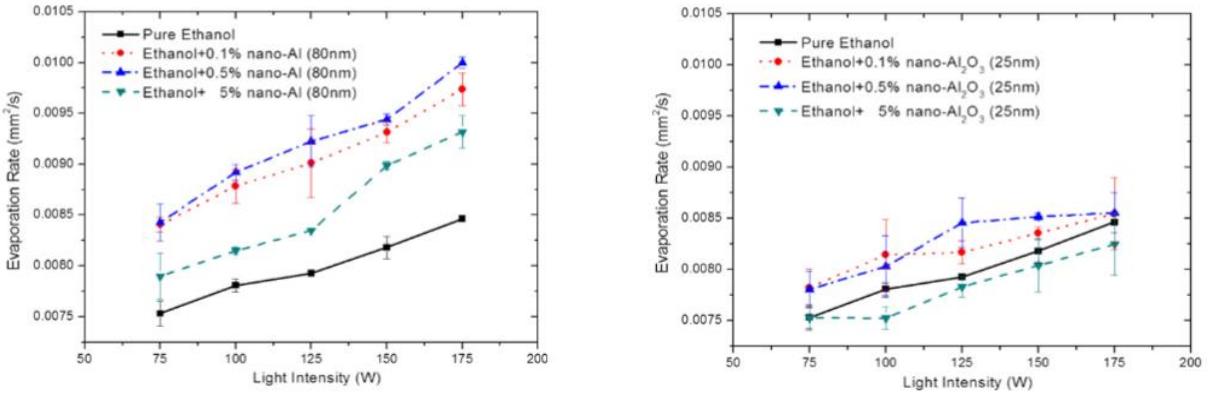

Figure 4: Variation in the evaporation rate with radiation intensity for aluminium-ethanol and aluminium oxide-ethanol of different concentrations (27)

Experiments on an Al-heptane nanofuel show a similar effect for temperatures below 400 °C, with an increase in particle loading rate causing a reduction in evaporation rate past a certain critical concentration due to the formation of agglomerates that inhibit evaporation (29). However, at temperatures above 400 °C, the evaporation rate was shown to increase with increased nanoparticle concentration up to a larger critical concentration, since the surfactant decomposed which resulted in small agglomerates that formed a porous shell that did not inhibit evaporation (29). The temperature-dependant aggregation mode of the nanoparticles has therefore been proven to be critical to the particle loading rate's effects on the evaporation rate (14). The nanofuel's convection mode also has a part to play, since it can also influence the particle aggregation. Under high forced convection, the D^2 Law was followed for fuels with aluminium additives. However, under low forced convection, aggregation of nanoparticles became more likely leading to departures from the D^2 Law and a decrease in evaporation rates (24).

The latent heat of vaporisation reducing due to the presence of nanoparticles is another proposed evaporation enhancement mechanism, since the evaporation constant λ of a fluid is inversely proportional to the latent heat of vaporisation as shown by the equations below (22):

$$\lambda = \frac{8k \cdot \ln(1+B)}{C_p \rho} \quad (2)$$

$$B = \frac{C_p(T_\infty - T_s)}{L} \quad (3)$$

$$\lambda \propto B \propto \frac{1}{L} \quad (4)$$

Evaporation enhancement is also achieved by microexplosions that occur at high temperatures due to nanoparticle agglomerates forming and heating residual base fuel droplets (22). The intense

separation of droplets caused by microexplosions increases evaporation rates due to the increase in surface area, which improves heat transfer from the hot surrounding gas to the droplet. They also encourage air-fuel mixing which improves burning, reducing emissions and fuel consumption. The flame disruption effects of nanoparticles being transported to the flame after microexplosion events may also encourage evaporation by increasing flame temperature (26).

Simply, droplet evaporation may also be enhanced by the packing of nanoparticles extending the base fluid surface area in contact with the hot environment (21).

3.2. Secondary Atomization Effects

Secondary atomization of burning nanofuels are made up of flame disruptive modes (20). Distinct modes of secondary atomization exist for both dilute nanoparticle concentrations and dense concentrations, that transport particles to the flame zone (15). Where dilute concentrations correspond to low intensity secondary atomization that cause local small flame distortions, dense concentrations cause intense bubble ejections, and more severe disruptions of flame envelopes (15). Alternatively, at particular low ejection intensities, daughter droplets that travel to the flame zone may simply vaporize rapidly, leaving nanoparticle aggregates (15). This section will first look at the classification of the nanofuel droplet secondary atomization phases, before considering mechanisms by which the presence of nanoparticles enhances evaporation including the microexplosion phenomenon.

3.2.1. Secondary Atomization Phases

Specific to nanofuels is the behaviour of secondary atomization through internal boiling and bubble ejection or bubble rupture (16) that then leads to ligament formation and ligament break up (15). These events can cause significant volumetric deformation in the droplet, specifically shape oscillations in a swell-shrink cycle. Two global indices are used to quantify bubble ejection behaviour (15):

Ejection impact parameter

$$\alpha_{global}(t) = \frac{\sum_{i=1}^{n} \frac{\pi}{6} {d_i}^3}{\frac{\pi}{6} D^3} = \alpha_{local,1} + \alpha_{local,2} + \cdots + \alpha_{local,n} \quad 5$$

Where n represents the bubble ejection frequency and d_i and D are the diameters of the ith bubble ejected and the combustion chamber parent droplet respectively. This parameter

represents the cumulative effects of the bubble ejections on the droplet's bulk shape deformation (15).

Droplet void fraction

$$\emptyset(t) = \sum_{j=1}^{N} \frac{{d_j}^3}{D^3} \qquad 6$$

Where *N* is the bubble population, and d_j and *D* are the diameters of *j*th bubble in the population and the parent droplet respectively. This parameter is an indirect measure of droplet pressure, and therefore determines the droplet's ability to undergo an ejection (15).

Low intensity minor bubble ejections are classified as $\alpha << 0.3$ whereas major bubble ejections that involve significant droplet undulations and large-scale shifting of the centroid are classified by $\alpha \rightarrow 1$. For a transient period before major droplet ejections, Darrieus Landau instability is seen where a single bubble and the parent droplet behave as a coupled system with in-phase oscillations (15).

In a study of the effects of nanotitania particles on ethanol-water fuel (15), the secondary atomization phases were found to comprise five modes that represent subregimes of minor and major droplet ejection as shown in Figure 5. They are as follows (15):

1. High kinetic energy pin or needle-type ligament ejections – ejection of thin ligaments that experience a series of fractures along their length ($\alpha_{local} << 0.01$ and $\emptyset = 0$).
2. Needle ejection with both tip and base breakup ($\alpha_{local} << 0.1$ and $\emptyset = 0$).
3. Low momentum ligaments with only tip break up ($0.1 < \alpha_{local} < 0.3$ and $0.1 < \emptyset < 0.2$).
4. Low momentum, thick ligament ejection ($\alpha_{local} > 0.3$ and $\emptyset > 0.3$).
5. Localised catastrophic fragmentation with multiple ligaments forming ($\alpha_{local} \rightarrow 1$ and $\emptyset \rightarrow 1$).

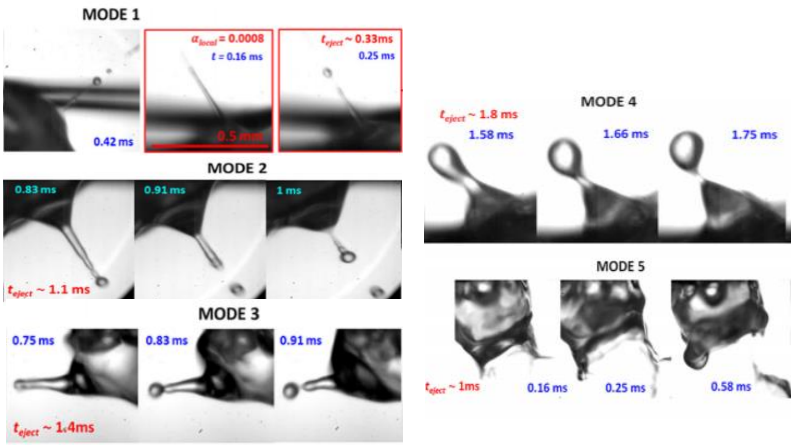

Figure 5: High speed images of the secondary atomization modes 1 – 5 (15).

The first three of these modes represent low intensity modes at dilute nanoparticle concentrations that introduce folds to the droplet surface, whereas the latter modes that dominate at high nanoparticle concentrations constitute high intensity bubble ejections that produce vigorous droplet surface undulations and bulk oscillations (15). Research has shown that at particularly dense particle loading rates, nanoparticle agglomeration may cause shell formation which sustains a pressure upsurge and reduces secondary atomization (15)(5). However, this may instead lead to microexplosion effects, which greatly enhance nanofuel burning rates (10). The likeliness of a microexplosion effect has been proven to increase with particle loading rate and temperature (14)(27). The effect of temperature is greater than that of particle loading rate (28).

3.2.2. Secondary Atomization Enhancement Mechanism

A study on the radiative heating of n-dodecane droplets containing cerium oxide nanoparticles of 0-0.5 wt% under acoustic levitation, three main secondary atomization mechanisms were described (16). For pure n-dodecane droplets, continuous 'pinching' of the parent droplet was seen, producing daughter droplets of 4-10 µm in diameter (16). This is secondary atomization due to Kelvin-Helmholtz instability – instability set in due to the relative motion between a droplet and its surroundings exceeding a critical value and thus inducing a shearing force on the surface.

Beyond a critical droplet size, secondary atomization can be seen to occur by catastrophic shattering due to extreme acoustic flattening. It occurs due to a rapid decrease in surface tension resulting from radiative heating of the droplet. A decrease in surface tension is significant since the droplet's stability is defined by the competing external pressure forces and internal restoring tension forces, quantified by the Weber number (We) (30):

$$We = \frac{\Delta p R_c}{\sigma} \qquad 7$$

Where Δp is the gradient in Bernoulli pressure between the droplet pole and equator, σ is the fluid surface tension and R_c is the droplet's equatorial radius of curvature. A decrease in surface tension therefore decreases the Weber number and increases droplet instability. Since radiative heating, which aids surface tension reduction, is enhanced by nanoparticles (27), nanofuels may be more susceptible to secondary atomization by catastrophic break up than pure fuels.

Catastrophic break up by acoustic flattening begins with an indent at the droplet pole (16). This indent then deepens progressively, which sees a major portion of liquid being transferred to the droplet periphery, resulting in a thin central membrane. The central region eventually ruptures,

causing further pressure accumulation in the rim which disintegrates and forms large daughter droplets (16). This same behaviour is not seen for pure ethanol droplets, since they experience greater evaporation rates and therefore a quicker regression in droplet diameter (16) resulting in We<1 and therefore greater stability. This secondary atomization mechanism therefore demonstrates a dependence on base fuel, droplet size and radiation intensity.

As mentioned previously, the primary enhancement mode offered by nanoparticles is an increase in nanoparticle aggregates that offer sites of bubble nucleation through internal boiling due to their heat absorption effect (31). A study of the effects of ceria nanoparticles on an ethanol-water base fuel found that at particle loading rates of 0.5% the bubble population is doubled and at 1.5% it is quadrupled (17). The modes of secondary atomisation through bubble ejection have been outlined in the previous subsection, but the mechanism of this behaviour comes in two forms as shown in Figure 6. One of these is intermittent bubble ejection at the free surface. The other is continuous bubble expansion as bubble coalesce and grow, and final disintegration of the droplet (16)(17).

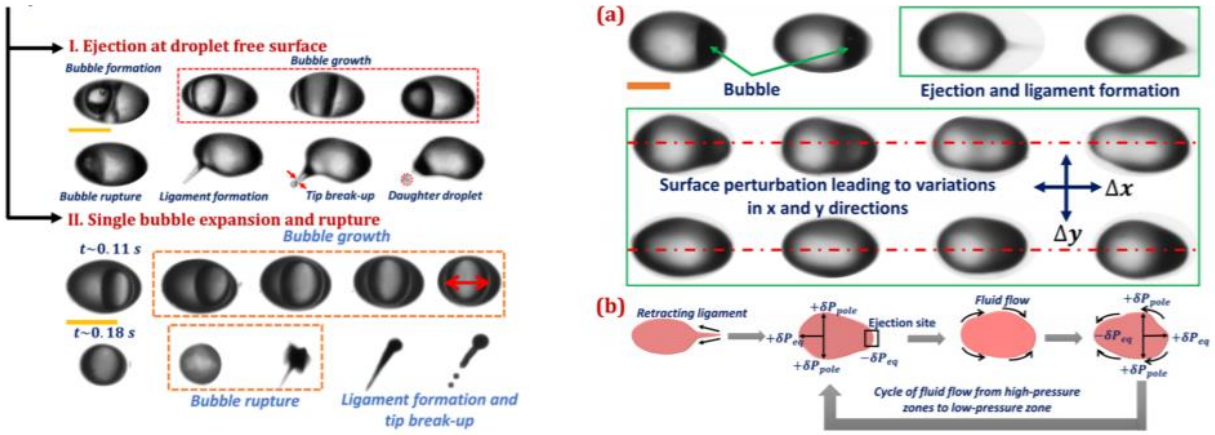

Figure 6: A representation of the two modes of internal boiling secondary atomization modes and the surface oscillation cycle following free surface ejection (16).

The bubble ejection pathway happens when the liquid film between the bubble and droplet boundary either undergoes thinning to the point of eventual rupture due to continuous growth, or surface shearing to the point of eventual rupture due to advancement to the liquid-air interface (17) (31). The surface opening due to the bubble collapse is a low-pressure crater, which the vicinal liquid rushes towards (16). This in flow generates liquid ligaments that break up at the tip through the Rayleigh-plateau mechanism. The excess energy of the liquid ligament that is retracted imparts a recoil force onto the droplet, which induces surface oscillations – undulation of the liquid droplet's surface in the vertical and horizontal directions are of the order ~10^{-2} mm (16) (17). As these waves travel across the droplet surface, they cause liquid to accumulate at the droplet

pole and on the opposite side of the equator to the bubble ejection zone, making them local high-pressure zones. Liquid then flows back to the original ejection location since there is now low pressure there once more. This cycle continues for 1-4 ms until the droplet is stabilised (16). Ejection events at the droplet pole result in even greater undulations and take longer to stabilise (~8 ms) (16).

On the other hand, the continuous bubble expansion and droplet disintegration pathway is characterised by minimal droplet shape distortion (16). Expansion continues until the bubble's characteristic length becomes comparable to that of the droplet. This thinning of the liquid layer between the bubble and droplet free surface results in eventual rupture at multiple locations (16).

Pressure upsurge occurs throughout the droplet during secondary atomization from internal boiling, due to bubble growth, bubble coalescence events and surface regression as gasification proceeds (5). This means that significant ligaments are released throughout (5). These are subjected to further Rayleigh-Plateau break-up events, forming daughter droplets that carry fuel to the flame envelope (17). As described, this may result in flame disruption or the depositing of nanoparticle aggregates that are ignited, increasing heat release. Either way, the gasification and atomization behaviour of the original parent droplet is affected, highlighting a coupled feedback loop (5)(17).

At low temperatures, past a certain particle loading rate, the increased aggregation of nanoparticles reduces the ejection events despite the increase in bubble population (14). This is due to the formation of a shell from the nanoparticle aggregates and the formation of vapour bends around the droplet as a result of the increase radiation absorption from the nanoparticles (5)(14). The shell sustains the pressure upsurge in the droplet and the vapour cloud reduces heat transferred to it, causing a decrease in burning rates due to decreased vaporisation and secondary atomization. At high temperatures however, shell agglomerates are more heterogeneous, leading to the phenomenon of microexplosions (14).

3.2.3. Microexplosion Effects

Aluminium-kerosene nanofuels have been investigated at concentrations of 2.5, 5.0, 7.5 wt% (32). At lower temperatures (400-500°C) microexplosion behaviour was only seen for the 5.0 and 7.0 wt% nanofuels. As temperatures increased further (600-800°C) microexplosion behaviour was seen for all three concentrations, but the microexplosions were more intense for the greater concentrations.

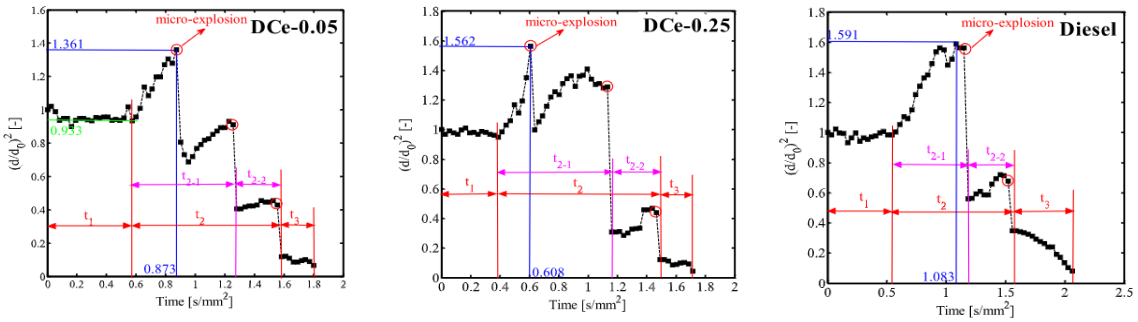

Figure 7: Variation in the droplet size with time for pure diesel and diesel with cerium oxide additives at concentrations of 0.05 wt% and 0.25 wt% (33).

As discussed, microexplosion behaviour significantly enhances the burning rate of nanofuel droplets. A study of pure diesel and cerium oxide nanoparticles added to diesel in concentrations of 0.05 wt% and 0.25 wt% (DCe-0.05 and DCe-0.25 respectively) by Wang et. al. found that, at 600°C, there are several sequential stages to the microexplosion phenomenon. The variation of the droplet size – the diameter squared – for the three fuels with time is shown in Figure 7, with both axes having been normalised by the original droplet diameter, d_0 (33).

The study found that, although all three fuels exhibit microexplosion behaviour, DCe-0.05 and DCe-0.25 exhibit three microexplosion processes where pure diesel exhibits two. For the DCe-0.05, the heat up stage continues until 0.510 s/mm^2, at which point, bubbles begin to form and continue to expand, before a microexplosion occurs at 0.873 s/mm^2. The droplet shape is then recovered, and expansion continues as more bubbles form, although less bubbles now form than before the first microexplosion. A second microexplosion occurs at 1.133 s/mm^2, and the series of processes repeat once more before a third microexplosion occurs at 1.493 s/mm^2. A steady state evaporation stage then ensues, which follows the D^2 Law. The DCe-0.25 fuel follows a similar mechanism, although the first microexplosion happens earlier and droplet expansion is greater than for the 0.05 wt% cerium concentration diesel. The DCe-0.25 also has a stronger secondary microexplosion, with the droplet expansion preceding it showing an amplitude similar to the droplet expansion seen before the first microexplosion (33).

The reason pure diesel exhibits microexplosions is due to the formation of first class bubbles. These are bubbles that form due to the gasification of low boiling point components in the nanofuel droplets. These small bubbles aggregate to form large bubbles which cause the droplets to continue to expand before eventually fragmenting. After this first microexplosion, only a small

portion of low boiling point components remain. The process repeats but the secondary microexplosion that occurs is less intense (33).

For DCe-0.05 and DCe-0.25 on the other hand, the presence of nanoparticles causes local hotspots in the fuel droplets, as the nanoparticles attain a temperature close to ambient temperature through radiation absorption. These spots act as nucleation sites of what are known as secondary class bubbles as the liquid near the nanoparticles are vaporized, whilst first class bubbles also form elsewhere in the fuel droplets. As well as two classes of bubbles forming instead of one, the rate of bubble formation is also increased relative to pure diesel by the fact that the increased temperatures brought about by the hotspots increased first class bubble formation. This increased bubble formation explains the greater intensity of microexplosions (33).

Although the overall evaporation rate is increased by the addition of nanoparticles (an increase of 16.6% and 25.2% compared to diesel for DCe-0.05 and DCe-0.25 respectively), the rate of evaporation during steady state evaporation phase which occurs after the microexplosion phase was shown to decrease (by 55.0% and 34.9% respectively). This is because the preceding droplet fragmentation causes the nanoparticle concentration in the droplets at this stage to be large. This causes a shell to form over the droplet that inhibits evaporation of the liquid fuel (33).

To quantify the effects of nanoparticle additives on microexplosion intensity, three parameters were defined: microexplosion intensity (Equation 8), expansion intensity (Equation 9) and the microexplosion delay (the time taken for a microexplosion to occur).

$$Microexplosion\ Intensity = \sum_{i=0}^{n} \frac{{d_{i2}}^2}{{d_{i3}}^2} \qquad 8$$

Where d_{i2} is the droplet diameter at the time when microexplosion occurs, d_{i3} is the diameter at the time when microexplosion ends, and *n* is the number of droplets.

$$Expansion\ Intensity = \sum_{i=0}^{n} \frac{{d_{i1}}^2}{{d_{i0}}^2} \qquad 9$$

Where d_{i1} is the maximum diameter of the droplet and d_{i0} is the diameter of the droplet when it just starts to expand.

For DCe-0.05 and DCe-0.25 respectively compared to diesel, the microexplosion intensity was shown to increase by 37.5% and 49.5%, the droplet expansion intensity by 21.8% and 35.1% and the microexplosion delay was shown to decrease by 24.1% and 47.1%. This demonstrates that

increasing the concentration of the cerium oxide nanoparticles in diesel results in more intense microexplosions, greater droplet expansion and quicker microexplosion occurrence (33).

3.3. Catalytic Effect

The catalytic effect of nanoparticles manifests in their aid of oxidation reactions. Metal nanoparticles have been shows to react with water, producing hydroxyl radicals that enhance soot or carbon atom oxidation (1). An attempt has also been made to develop nanoparticles that act as three-way catalysts (34), by catalysing the following transitions:

$$Carbon\ Monoxide\ (CO) \rightarrow Carbon\ Dioxide\ (CO_2)$$

$$Hydrocarbons\ (HC) \rightarrow Water\ (H_2O)$$

$$Oxides\ of\ Nitrogen\ (NO_{x)}\ \rightarrow Nitrogen\ (NO_2)$$

The study involved the preparation of a stable dispersion of surfactant-coated Ce-Zr nanoparticles in diesel. The three-way catalyst's dominant effect under fuel-rich conditions was to provide oxygen to CO and HC, and under fuel lean conditions it was to extract O_2 from NO_x. The natural oxygen storing capacity of CeO_2 was made use of, with the Zr being added as a doping agent to further improve this capacity whilst also improving the thermal stability. The addition of Zr in the cerium lattice achieved this effect by creating bulk defects that provide pathways for better oxygen migration rates. The maximum oxygen storing capacity of the mixture was shown to occur for 60% to 70% Ce (34).

3.4. Discussion of Combustion Mechanism

From the results discussed, it can be concluded that, at low temperatures, evaporation is aided by increasing nanoparticle concentrations to a point due to increased radiative absorption, beyond which the evaporation rate and secondary atomization effects are decreased due to shell formation (15)(27). At high temperatures however, surfactant decomposition may result in smaller nanoparticle agglomerates and therefore porous shell formation, which removes this inhabitation effect (35). At temperatures significantly beyond the boiling point of the base fuel, there are significant droplet fragmentation effects at the start of the heat-up phase, as well as microexplosion effects towards the ends of the steady state phase, due to shells causing second class bubble formation (33) and pressure build up due to nanoparticle agglomerates heating up residual fuel droplets (26). This droplet fragmentation and microexplosion behaviour greatly enhances the evaporation rate of the nanofuel droplets, shortening ignition delay (12). It is aided

by increasing the nanoparticle concentrations further so that shells can form more easily, and agglomerates are larger.

Other than microexplosions, three mechanisms for secondary atomization have been considered: Kelvin-Helmholtz instability, catastrophic shattering and internal boiling that involves bubble ejection and bubble expansion (16). The increasing of the nanoparticle loading rate, before a critical concentration if there is one for the temperature range being considered, is seen to enhance secondary atomization by the internal boiling mechanism due to increased radiation absorption (27).

Since an increase in the Weber number, which defines the catastrophic break-up mechanism of secondary atomization, is caused by a reduction of surface tension induced by an increase in the radiation absorption of the fuel droplet, it is reasonable to assume that increasing the particle loading rate should aid this mechanism also. However, Pandey and Basu have found that particle loading rate does not affect this mechanism (16). The same study also found that neither pure nor particle laden nanofuel droplets of ethanol fuel exhibit any secondary atomization whatsoever (16), where other studies have seen secondary atomization following surface crater formation in ethanol-water due to surface regression from vaporisation and the surface tension becoming imbalanced as defined by the Weber number (17). These characteristics should therefore be investigated further.

A complex relationship exists between radiation intensity and bubble nucleation. Increasing particle loading rates increases bubble nucleation due to agglomerate formation allowing for greater radiation absorption. However, increasing the intensity of a laser incident upon the droplets decreases bubble nucleation due to the fact that the enhanced evaporation rate decreases the droplet's lifetime, and therefore decreases the ability for nanoparticles to agglomerate (16). This suggests that, to maximise bubble nucleation and hence secondary atomization intensity, the radiation absorption of the droplet must be increased by encouraging particle agglomeration rather than by directly increasing the incident radiation, which would introduce the adverse effect of reducing radiation absorption by preventing aggregation. Still, the relationship between nanoparticle addition and bubble formation is contentious, where some research has suggested that increasing nanoparticle concentration increases bubble formation, the addition of aluminium nanoparticle to heptane fuel has been reported to suppress bubble formation (29).

4. Engine Performance and Emissions

Table 1: Engine performance and emissions with various base fuels, nanoparticle additives, engine types and operating conditions (8) (and references therein).

Base fuel	Engine	Operating condition	Nano fluid additive	Composition	Performance results	Emission results
Jatropha biodiesel Water emulsion	1-Cylinder, AC, NA, 4 stroke, DI	1500 rpm, different load, constant injection timing	Aluminum oxide (Al_2O_3)	25, 50, 100 ppm	Increased BTE, lower BSFC	Lower NO_x, HC, smoke opacity Slightly higher CO,
Diesel	4-Cylinder, WC, TC, 4 stroke, DI	1000–3000 rpm	Titanium oxide (TiO_2)	0.20%	Higher BP, lower BSFC	Lower NO_x, CO and CO_2
Diesel	1-Cylinder, WC, NA, 4 stroke, DI	1500 rpm, different load	Cerium oxide	5–40 ppm	Increased BTE	Lower NO_x, HC
Jatropha biodiesel	1-Cylinder, WC, NA, 4 stroke, DI	1500 rpm, different load	Cerium oxide	20–80 ppm	Improved BTE	Reduced HC, NO_x, Slightly reduced CO
Jatropha biodiesel Water emulsion	1-Cylinder, AC, NA, 4 stroke, DI	1500 rpm, different load, constant injection timing	Aluminium oxide (Al_2O_3)	25, 50, 100 ppm	Increased BTE, lower BSFC	Lower NO_x,HC, smoke opacity slightly higher CO
Jatropha biodiesel	1-Cylinder, AC, NA, 4 stroke, DI	Load 25, 50, 75, 100%	Magnalium (Al–Mg) Cobalt oxide (Co_3O_4)	100 mg/l	Reduction in BSEC, improvement in BTE	Reduced HC, NO_x and CO
Waste cooking palm oil	1-Cylinder, WC, NA, 4 stroke, DI	220, 280 bar IP, 230°, 25.5° Btdc IT, Load 25, 50, 75, 100%, 1500 rpm	Ferric chloride ($FeCl_3$)	5–50 μmol/l	Lower BSFC, BSEC Higher BTE	Higher CO, NO_x lower HC, smoke opacity
Diesel	4-Cylinder, WC, IL, 4 stroke, DI	2200 rpm	Ferrofluid (Fe_3O_4)	0.4%, and 0.8% by volume	Decreased BSFC and increased BTE	Reduction in NO_x Higher CO
Jatropha biodiesel	1-Cylinder, AC, NA, 4 stroke, DI, 215 bar IP	1500 rpm, different load, constant injection timing 26°bTDC	Aluminium oxide (Al_2O_3) Carbon nano-tube (CNT)	25, 50 ppm	Decreased BSFC and increased BTE	Lower HC, CO, NO_x smoke opacity
Diesel	1-Cylinder, WC, NA, 4 stroke, DI, 17° IT	40–15 N-m Torque 1200–2400 rpm	aluminum nano-particles(Al)	30–50 cc	Lower BSFC at 1200 and 1800 rpm but no change at 2400 rpm.	Lower NO_x ,smoke at 1200 and 1800 rpm but no change at 2400 rpm.
Diesel-biodiesel-ethanol blends	1-Cylinder, 4 stroke, Variable Compression ratio, WC	At 19 CR,0.44 MPa, 1500 rpm	Cerium oxide	25 ppm	Lower BSFC, improvement in BTE	Lower CO, HC and smoke higher NO_x
Diesel	1-Cylinder, AC, NA, 4 stroke, DI	25–100% load, 1500 rpm	Manganese oxide (MnO) Copper oxide (CuO)	200 mg/l	Increased BTE	Lower NO_x CO, HC.Manganese oxide better than Copper oxide
Diesel	1-Cylinder, WC, NA, 4 stroke, DI	1500 rpm, different load,	Aluminum Iron Boron	0.5 wt%	Marginal increase in BSFC at lower load in Al and Boron. No variation in Iron. Drop in BSFC at higher load for Al. Rise in exhaust gas temperature for all. Better BTE at all loads.	CO and HC increased for Al and iron at lower loads and reduced at higher loads. Boron showed same trends as diesel. Higher NO_x and soot for Al and iron
Diesel–biodiesel–ethanol blends	1-Cylinder, 4 stroke, variable compression ratio, NA, WC	0–100% load and 1500 rpm	Cerium oxide Carbon nanotube	25, 50, 100 ppm 25, 50, 100 ppm	Decreased BSFC and increased BTE	Higher concentration decreased NO_x, HC and smoke and increased CO
Water–diesel emulsion	1-Cylinder, WC 4 stroke, DI	Various load and 1500 rpm	nano-silicon (n-Si) nano-aluminum	0.1%	Lower BSFC and Higher BTE	Higher NO_x, HC and lower CO at lower load

By the mechanisms explained in the previous section, nanofuels have the potential to shorten ignition delay, increase burning rates and encourage rapid oxidation. The burning may also see a greater heat release since the high energy density of the nanoparticles increase the calorific value of the fuel (8). The use of nanofuels in an engine can therefore increases power output (6). However, the true effect of nanofuels on engine performance and emissions depends on the relative strength of several interacting conditions, including ambient temperature, pressure and radiation level, as well as base fuel and nanoparticle type, particle loading rate and surfactant use (20). The operating condition as defined by the engine loading is also critical. Table 1 below shows findings by various researchers on nanofuel use in engines.

4.1. Aluminium Nanoparticles

A study of aluminium, boron and carbon nanoparticles added to diesel fuel used in a CI engine have shown positive effects (6). The ignition probability was increased at lower temperatures for each case, thereby reducing the ignition time from ~1.2 s for pure diesel to ~0.2 s. The brake thermal efficiency was increased for the use of all three nanofuels, with the greatest increase of 9% being seen for aluminium nanoparticle additives, as well as a 7% reduction in specific fuel

consumption. However, at higher loads, the 8% increase in the exhaust gas temperature resulted in a 5% increase in NOx emission compared to pure diesel due to enhanced oxidation rates. Hydrocarbon and CO emissions on the other hand decreased by 8% and 40% respectively. The impact of engine loading on aluminium-diesel burning is confirmed to be significant by a study that found brake specific energy consumption to be higher than pure diesel at 25% and 50% load but less at 75% (36).

Another study looked at the engine performance effects of aluminium additives to an ethanol base fuel (37). Above 3 wt% aluminium, the amount of heat released was found to increase almost linearly, with aluminium concentrations of 10% increasing the heat of combustion by 15.3%. Addition of aluminium oxide nanoparticles on the other hand did not influence the heat of combustion since, being inert, they did not participate in the combustion reactively. Their poor radiation absorption also explains why they did not enhance combustion as explain in Section 3.1. However, emissions have been shown to decrease at 0.5% aluminium oxide, with a maximum reduction in hydrocarbons and CO_2 of 25% and 32.8% respectively being observed (38). Aluminium added to another biofuel, Jathropa, has also shows positive results, with a reduction of 9%, 17%, 33% and 20% of NO, smoke opacity, unburnt HC and CO respectively, and an increase in brake thermal efficiency of 5% (39).

Kerosene droplets with 0.1 wt% and 1 wt% aluminium were studied at different ambient pressures in the range 0.1-2.5 MPa and different ambient temperatures in the range 400-700°C (40). Both concentrations showed exponentially decreasing ignition delay time with temperatures. As ambient pressure increased, the ignition delay first decreased as the heat of vaporization decreased before increasing again due to high pressures inhibiting the ability for the fuel vapour to diffuse and mix with the air sufficiently. It was also found that as the ambient pressure increased, the lowest temperature for the onset of ignition increased from 800 °C at 0.1 MPa to 400 °C at 2.5 MPa. At pressures greater than 1 MPa, the ignition delay of droplets with 1 wt% aluminium was consistently shorter than that of both pure kerosene and kerosene with 0.1 wt% aluminium regardless of ambient temperature. The ignition delay of 0.1 wt% aluminium for this range of pressures was consistently greater than pure kerosene.

4.2. Cerium Oxide Nanoparticles

The addition of cerium oxide nanoparticles is popular due to the catalytic effect it contributes to reduce the brake specific fuel consumption and increase brake thermal efficiency (41). The

additive has an oxygen buffering capability, whereby it simultaneously catalyses the reduction of NOx and the oxidation of unburnt hydrocarbons (42). One study found that the addition of 30 ppm of cerium oxide to biodiesel increased the brake thermal efficiency by 1.7% and reduced NOx emission by 7% compared to pure biodiesel (43). This positive effect is corroborated by the addition of cerium oxide to Jathropa biodiesel resulting in a reduction in emissions of NO, smoke opacity, unburnt hydrocarbons and CO by 7%, 20%, 28% and 20% respectively. This study also found a thermal efficiency increase compared to pure Jathropa at 5% (39). However, the oxidative stability of biodiesels when cerium oxide nanoparticles are added is seen to decrease, demonstrated by a reduction in the induction period by 45% at 100 ppm (41).

The positive catalytic effect of cerium oxide is also seen when it is added to a diesel base fuel, with a fuel saving of 10% being reported (41). However, a limiting concentration for trends in brake thermal efficiency as cerium oxide doping is increased has been shown (42). A maximum brake thermal efficiency enhancement compared to pure diesel of 5% is seen, corresponding to a reduction of HC and NOx emissions by 45% and 30% respectively, but beyond 35 ppm cerium oxide there is a slight decrease in brake thermal efficiency due to the increased chance of agglomeration, hindering combustion mechanisms as discussed in the previous section. Nevertheless, at 35 ppm, a positive trend was realised in the concentration of dodecyl succinic anhydride surfactant and brake thermal efficiency, especially at high loads (42). Yet there is a limit to the enhancement offered by increasing surfactant concentration also, with a drop in efficiency observed when surfactant concentration is increased to 5%.

Studies have been conducted into the effect on engine performance of combining both cerium oxide nanoparticle and carbon nanotube additives. The brake thermal efficiency when the two additives were each used at 100 ppm in a diesel-biodiesel-ethanol blend was found to increase by 8.05% (43). However, a separate study found that using the two additives at 50 ppm each resulted in an increase in CO emission by 22.2%. Nevertheless, hydrocarbon and smoke emissions were seen to decrease by 7.2% and 47.6% respectively (44). In Section 3.1. it was mentioned that the addition of zirconium to cerium oxide can be used to enhance its catalytic performance. Studies have found a resulting decrease in smoke emission by 31% and an increase in thermal efficiency by 3% (3).

4.3. Other Nanoparticles

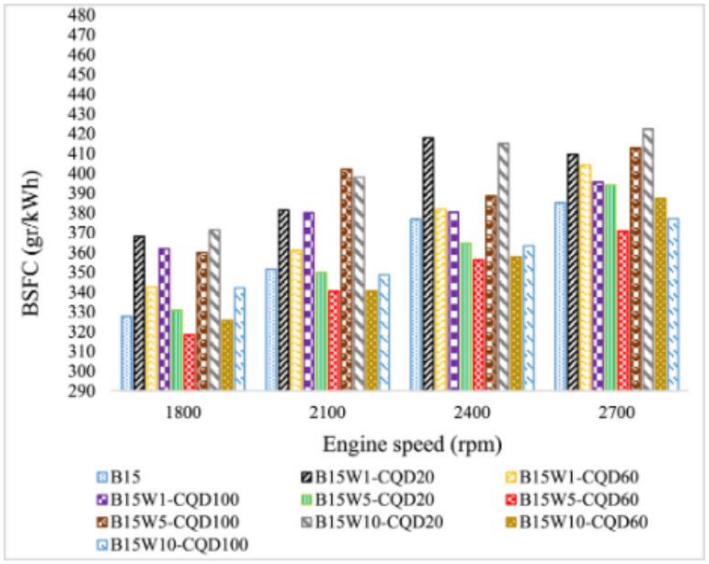

Figure 8: Brake specific fuel consumption for different blends of diesel-biodiesel-water-carbon quantum dot nanoparticles as load is varied (3).

Water and biodegradable carbon quantum dot nanoparticles were added to a diesel-biodiesel fuel blend in order to alleviate the toxicity and stability concerns present with other nanoparticles (3). The additives, at 5% water and 60 ppm carbon quantum dot nanoparticles, increased the diesel engine power output at maximum load by 21%. A range of ten different water and carbon quantum dot compositional combinations studied revealed that the concentration of each had a significant effect on engine performance and emission. For 10% water with 20 ppm nanoparticle, 1% water with 20 ppm nanoparticles, 5% water with 100 ppm nanoparticles and 1% water with 100 ppm nanoparticles, the brake specific fuel consumption was found to consistently be significantly greater than that of diesel for any loading, as shown by Figure 8. However, the addition of any compositional combination of water and nanoparticle decreased NOx emissions. The effect on hydrocarbon emission was a marginal decrease for most combinations at most loads, and the effect on CO emission followed no particular trend (3).

The addition of graphene oxide nanoparticles to a CI engine fuelled with dairy scum oil biodiesel notable enhanced the engine performance and emission characteristics, resulting in a reduction in combustion duration and ignition delay. The brake thermal efficiency was shown to increase by 11.6%, with a reduction in brake specific fuel consumption of 8.3%. Unburnt hydrocarbon, smoke, CO and NOx emissions were all reduced by 21.7%, 24.9%, 38.7% and 5.6% respectively (45).

4.4. Discussion of Engine Performance and Emissions

Although most research points to the potential for nanoparticles to increase the brake thermal efficiency, the engine parameter of cylinder pressure has been proven more contentious. The cylinder pressure when aluminium is added to diesel is found to decrease by Mehta et al. (6), but the opposite effect is reported by both Khond and Kriplani (8) and Shaafi and Velraj (36). Furthermore, for aluminium nanoparticles in Jathropa biodiesel, the cylinder pressure is seen to fall (39) whilst for cerium oxide in a diesel-biodiesel blend, an increase in cylinder pressure is claimed (44).

The stability of nanofuels is of concern, in particular the oxidative stability of cerium oxide additives effects its catalytic ability. To ensure this stability, concentrations of antioxidants are required, which decrease the size of the nano cerium oxide particles and increase the oxygen absorbance potential (41). However, the presence of the antioxidant may itself impart effects on engine performance and emissions, as has been found with most research into nanofuels that use surfactants (42).

A study that used Envirox – a commercial nano ceria additive – in diesel found that at the manufacturer recommended concentration, the number of ultrafine particles in the engine exhaust increased by 32% (despite a 24% decrease by mass) (46). This is believed to be the result of the breakdown of nanoparticle agglomerates caused by the soot oxidative process. A decrease in particulate emission size poses a significant health risk that must be further investigated. The negative health effect of nanoparticle use is compounded by their potential to increase emission of harmful NOx, here increasing emissions by 9.3% despite a reduction in CO emissions by 10.6% (46). It should be noted however that this contradicts other research which has found that, in the case of ceria nanoparticles, there is no significant effect on NOx emissions (47).

5. Limitations of Nanofuels

Concerns surrounding nanofuel use include stable preparation, the optimization of combustion parameters, health and safety concerns, environmental impacts, ease of nanoparticle regeneration and potential damage to engines (48).

As seen in the previous section, there are few unifying trends on the optimising of parameters for engine performance and emissions. The specific nanofuel being used must therefore be studied in

detail before its use in an engine with consideration given to nanoparticle concentration and shape, surfactant concentration, ambient conditions and engine operating conditions (16). The increase in NOx emission seen in many nanofuel applications is concerning from a health and environmental perspective, though significant potential reduction in other hazardous emissions is encouraging (12). The emission of particulate matter as metal oxides or unburnt nanoparticles has potentially damaging pulmonary effects. A study that exposed groups of rats to either diesel exhaust (DE) or diesel with cerium oxide additive exhaust (DECe) observed greater lung injury biomarkers in the DECe group (49). The fact that when metal or metal oxide nanoparticles are released into the environment, there is no physiochemical change for a long time is also of concern (12). A few methods have therefore been developed to collect nanoparticles from emissions, which may also prove beneficial for regeneration of nanoparticles for re-use, but each of these have an attached cost. Collection by mechanical forces have been attempted by means of a cyclone or impactor, but this has proved inefficient as nanoparticles follow the motion of their carrying gas (48). Electrostatic forces have proven an effective separation method for bigger particles, but for additives of the nano scale, the low charge probability may make this method redundant (48). Magnetic mechanisms are successful provided the nanoparticle has sufficient magnetic properties. Filtration is also effective, with high efficiency particulate air filters that are used in the nuclear industry providing 99.99% collection efficiency, though they are costly and would present a challenge in removing nanoparticles and oxides from the filter for reuse (48).

The difficult in achieving effective stability presented by the tendency for nanoparticles to agglomerate in another challenge. Not only does agglomeration disrupt the combustion characteristics of the fuel as discussed, it shortens its shelf-life and potentially presents lubrication and wear problems to engine (13). Non-uniformly dispersed additives may also lead to unpredictable spray behaviour from the fuel injector system (48).

6. Discussion and Conclusion

This literature review has found a diversity of effects on combustion behaviour of nanoparticle addition to fuels. This suggests that nanofuels offer freedom to tailor a fuel to enhance targeted effects. The control of the physiochemistry is an exciting prospect, since different applications may require the optimisation of different specific effects on the local or global combustion scale to influence general or specific combustion behaviour respectively. Behaviour that might be targeted

may include reduction of certain emissions or fuel consumption, or enhancement of thermal efficiency, stability, evaporation rates, bubble ejection or microexplosion intensity

However, further research into this field is first required to overcome certain challenges and to better understand behavioural effects. In preparing nanofuels, the one-step method seems to present an advantage over the current staple two-step method. In creating the nanoparticles and dispersing them in the base fuel simultaneously, this method would potentially eliminate steps in the preparation process such as drying, storage and transportation of nanoparticles. Nevertheless, the issue with this method is that the residual reactants left in the fuel after reactions to produce nanoparticles are impurities that may alter the fuel's combustion behaviour. The same can be said for surfactants, that have shown trends in altering combustion behaviour with concentration. Further research should be conducted into methods of removing the effects of impurities or surfactants or identifying trends to find their optimum concentration and ratio to the nanoparticle concentration for enhancement of the targeted behaviour.

Being a relatively novel field, certain contradiction or disagreement exists in the literature. The influence of nanoparticles on the chamber pressure is one of these. This is a significant concern for applications where chamber pressure is limited due to engine material constraints for example. The variation of the effect on NOx emission is another contentious topic, although the majority of nanofuels tested in literature demonstrate a potential increase. Those nanofuels that do not increase NOx emissions should be researched further to gain an understanding for why that it is the case. Furthermore, research that has suggested nanoparticles do not have an effect on the catastrophic break up mechanism of nanofuels should also be investigated further. Due the reduction of surface tension that nanoparticles' radiation absorption enhancement encourages, it is expected that some effect should be seen.

In conclusion, this literature review has considered the preparation of nanofuels, their effect on local droplet behaviour in the combustion chamber, the global effect on engine performance and emissions, and limitations of their use. It is suggested that the field be researched further to formalise a qualitative or quantitative classification of the trends in effects with the range of relevant parameters for any given nanofuel.

References

(1) Lenin MA, Swaminathan MR, Kumaresan G. Performance and emission characteristics of a DI diesel engine with a nanofuel additive. *Fuel.* 2013; 109 362-365. Available from: doi: 10.1016/j.fuel.2013.03.042 Available from: http://dx.doi.org/10.1016/j.fuel.2013.03.042 .

(2) Soudagar MEM, Nik-Ghazali N, Kalam MA, Badruddin IA, Banapurmath NR, Yunus Khan TM, et al. The effects of graphene oxide nanoparticle additive stably dispersed in dairy scum oil biodiesel-diesel fuel blend on CI engine: performance, emission and combustion characteristics. *Fuel.* 2019; 257 Available from: doi: 10.1016/j.fuel.2019.116015 Available from: http://dx.doi.org/10.1016/j.fuel.2019.116015 .

(3) Ettefaghi E, Ghobadian B, Rashidi A, Najafi G, Khoshtaghaza MH, Rashtchi M, et al. A novel bio-nano emulsion fuel based on biodegradable nanoparticles to improve diesel engines performance and reduce exhaust emissions. *Renewable Energy*. 2018; 125 64-72. Available from: doi: 10.1016/j.renene.2018.01.086 Available from: http://dx.doi.org/10.1016/j.renene.2018.01.086 .

(4) Saxena V, Kumar N, Saxena VK. A comprehensive review on combustion and stability aspects of metal nanoparticles and its additive effect on diesel and biodiesel fuelled C.I. engine. *Renewable and Sustainable Energy Reviews.* 2017; 70 563-588. Available from: doi: 10.1016/j.rser.2016.11.067 Available from: http://www.sciencedirect.com/science/article/pii/S1364032116308012 [Accessed Oct 26, 2019].

(5) Basu S, Miglani A. Combustion and heat transfer characteristics of nanofluid fuel droplets: A short review. *International Journal of Heat and Mass Transfer.* 2016; 96 482-503. Available from: doi: 10.1016/j.ijheatmasstransfer.2016.01.053 Available from: http://www.sciencedirect.com/science/article/pii/S0017931015311601 [Accessed Oct 26, 2019].

(6) Mehta RN, Chakraborty M, Parikh PA. Fuel. *Fuel.* 1948; 120 91-97. Available from: http://www.sciencedirect.com/science/article/pii/S0016236113011459 .

(7) Ghanbari M, Najafi G, Ghobadian B, Yusaf T, Carlucci AP, Kiani DK. Performance and emission characteristics of a CI engine using nano particles additives in biodiesel-diesel blends and modeling with GP approach. *Fuel.* 2017; 202 699-716. Available from: doi: 10.1016/j.fuel.2017.04.117 Available from: http://dx.doi.org/10.1016/j.fuel.2017.04.117 .

(8) Khond VW, Kriplani VM. Effect of nanofluid additives on performances and emissions of emulsified diesel and biodiesel fueled stationary CI engine: A comprehensive review. *Renewable and Sustainable Energy Reviews.* 2016; 59 1338-1348. Available from: doi: 10.1016/j.rser.2016.01.051 Available from: http://www.sciencedirect.com/science/article/pii/S1364032116000812 [Accessed Oct 26, 2019].

(9) Zhao N, Zheng H, Wen X. Research progress on liquid nanofuel and its combustion enhancement. *Huagong Jinzhan/Chemical Industry and Engineering Progress*. 2018; 37 (4): 1364-1373. Available from: doi: 10.16085/j.issn.1000-6613.2017-1139 Available from: http://dx.doi.org/10.16085/j.issn.1000-6613.2017-1139 .

(10) Shaafi T, Velraj R. Influence of alumina nanoparticles, ethanol and isopropanol blend as additive with diesel–soybean biodiesel blend fuel: Combustion, engine performance and emissions. *Renewable Energy.* 2015; 80 655-663. Available from: doi: 10.1016/j.renene.2015.02.042 Available from: https://www.sciencedirect.com/science/article/pii/S0960148115001585 .

(11) Keskin A, Gürü M, Altıparmak D. Biodiesel production from tall oil with synthesized Mn and Ni based additives: Effects of the additives on fuel consumption and emissions. *Fuel.* 2007; 86 (7): 1139-1143. Available from: doi: 10.1016/j.fuel.2006.10.021 Available from: http://www.sciencedirect.com/science/article/pii/S0016236106004418 [Accessed Nov 28, 2019].

(12) Abdel-Rehim A, Akl S. An Experimental Investigation of the Effect of Aluminum Oxide (Al 2 O 3) Nanoparticles as fuel additive on the Performance and Emissions of a Diesel Engine. 2016; Available from: doi: 10.4271/2016-01-0828 [Accessed Nov 28, 2019].

(13) Yu W, Xie H. *A Review on Nanofluids: Preparation, Stability Mechanisms, and Applications.* Available from: https://www.hindawi.com/journals/jnm/2012/435873/ [Accessed Dec 12, 2019].

(14) Wang X, Zhang J, Ma Y, Wang G, Han J, Dai M, et al. Applied surface science. *Applied surface science.* 1985; 144581. Available from: http://www.sciencedirect.com/science/article/pii/S0169433219333975 .

(15) Miglani A, Basu S. Effect of Particle Concentration on Shape Deformation and Secondary Atomization Characteristics of a Burning Nanotitania Dispersion Droplet. *Journal of Heat Transfer.* 2015; 137 (10): Available from: doi: 10.1115/1.4030394 Available from: https://asmedigitalcollection.asme.org/heattransfer/article/137/10/102001/383864/Effect-of-Particle-Concentration-on-Shape [Accessed Nov 24, 2019].

(16) Pandey K, Basu S. How boiling happens in nanofuel droplets. *Physics of Fluids.* 2018; 30 (10): 107103 (12 pp.). Available from: doi: 10.1063/1.5048564 [Accessed Dec 4, 2019].

(17) Pandey K, Basu S. High vapour pressure nanofuel droplet combustion and heat transfer: Insights into droplet burning time scale, secondary atomisation and coupling of droplet deformations and heat release. *Combustion and Flame.* 2019; 209 167-179. Available from: doi: 10.1016/j.combustflame.2019.07.043 Available from: http://www.sciencedirect.com/science/article/pii/S0010218019303530 [Accessed Dec 4, 2019].

(18) Missana T, Adell A. On the Applicability of DLVO Theory to the Prediction of Clay Colloids Stability. *Journal of Colloid And Interface Science.* 2000; 230 (1): 150-156. Available from: doi: 10.1006/jcis.2000.7003 Available from: https://www.sciencedirect.com/science/article/pii/S0021979700970036 .

(19) Zhu H, Lin Y, Yin Y. A novel one-step chemical method for preparation of copper nanofluids. *Journal of Colloid and Interface Science.* 2004; 277 (1): 100-103. Available from: doi: 10.1016/j.jcis.2004.04.026 Available from: http://www.sciencedirect.com/science/article/pii/S0021979704003893 [Accessed Dec 12, 2019].

(20) Emekwuru NG. Nanofuel Droplet Evaporation Processes. *Journal of the Indian Institute of Science.* 2018; 99 43-58. Available from: doi: 10.1007/s41745-018-0092-2 [Accessed Dec 4, 2019].

(21) Chen R, Phuoc TX, Martello D. International journal of heat and mass transfer. *International journal of heat and mass transfer.* 1960; 53 (19): 3677-3682. Available from: http://www.sciencedirect.com/science/article/pii/S0017931010001900 .

(22) Emekwuru NG. Nanofuel Droplet Evaporation Processes. *Journal of the Indian Institute of Science.* 2019; 99 (1): 43-58. Available from: doi: 10.1007/s41745-018-0092-2 Available from: http://dx.doi.org/10.1007/s41745-018-0092-2 .

(23) Godsave GAE. Studies of the combustion of drops in a fuel spray—the burning of single drops of fuel. *Symposium (International) on Combustion.* 1953; 4 (1): 818-830. Available from: doi: 10.1016/S0082-0784(53)80107-4 Available from: https://www.sciencedirect.com/science/article/pii/S0082078453801074 .

(24) Gan Y, Qiao L. Evaporation characteristics of fuel droplets with the addition of nanoparticles under natural and forced convections. *International Journal of Heat and Mass Transfer.* 2011; 54 (23): 4913-4922. Available from: doi: 10.1016/j.ijheatmasstransfer.2011.07.003 Available from: https://www.sciencedirect.com/science/article/pii/S0017931011003796 .

(25) Javed I, Baek SW, Waheed K, Ali G, Cho SO. Evaporation characteristics of kerosene droplets with dilute concentrations of ligand-protected aluminum nanoparticles at elevated temperatures. *Combustion and Flame.* 2013; 160 (12): 2955-2963. Available from: doi: 10.1016/j.combustflame.2013.07.007 Available from: http://www.sciencedirect.com/science/article/pii/S0010218013002654 [Accessed Nov 21, 2019].

(26) Sim HS, Plascencia MA, Vargas A, Bennewitz JW, Smith OI, Karagozian AR. Effects of Inert and Energetic Nanoparticles on Burning Liquid Ethanol Droplets. *Combustion Science and Technology.* 2019; 191 (7): 1079-1100. Available from: doi: 10.1080/00102202.2018.1509857 Available from: https://doi.org/10.1080/00102202.2018.1509857 .

(27) Gan Y, Qiao L. Radiation-enhanced evaporation of ethanol fuel containing suspended metal nanoparticles. *International Journal of Heat and Mass Transfer.* 2012; 55 (21-22): 5777-5782. Available from: doi: 10.1016/j.ijheatmasstransfer.2012.05.074 Available from: https://www.sciencedirect.com/science/article/pii/S001793101200395X .

(28) Javed I, Baek SW, Waheed K. Effects of dense concentrations of aluminum nanoparticles on the evaporation behavior of kerosene droplet at elevated temperatures: The phenomenon of microexplosion. *Experimental Thermal and Fluid Science.* 2014; 56 33-44. Available from: doi: 10.1016/j.expthermflusci.2013.11.006 Available from: http://www.sciencedirect.com/science/article/pii/S0894177713002483 [Accessed Nov 24, 2019].

(29) Javed I, Baek SW, Waheed K. Combustion and flame. *Combustion and flame.* 1957; 160 (1): 170-183. Available from: http://www.sciencedirect.com/science/article/pii/S0010218012002568 .

(30) Basu S, Saha A, Kumar R. Criteria for thermally induced atomization and catastrophic breakup of acoustically levitated droplet. *International Journal of Heat and Mass Transfer.* 2013; 59 316-327. Available from: doi: 10.1016/j.ijheatmasstransfer.2012.12.040 Available from: http://www.sciencedirect.com/science/article/pii/S0017931012009969 [Accessed Dec 4, 2019].

(31) Pandey K, Chattopadhyay K, Basu S. Combustion dynamics of low vapour pressure nanofuel droplets. *PhFl.* 2017; 29 (7): 074102. Available from: doi: 10.1063/1.4991752 Available from: https://ui.adsabs.harvard.edu/abs/2017PhFl...29g4102P/abstract [Accessed Dec 4, 2019].

(32) Javed I, Baek SW, Waheed K. Experimental thermal and fluid science. *Experimental thermal and fluid science.* 1988; 56 33-44. Available from: http://www.sciencedirect.com/science/article/pii/S0894177713002483 .

(33) Wang J, Qiao X, Ju D, Wang L, Sun C. Experimental study on the evaporation and micro-explosion characteristics of nanofuel droplet at dilute concentrations. *Energy.* 2019; 183 149-159. Available from: doi: 10.1016/j.energy.2019.06.136 Available from: http://www.sciencedirect.com/science/article/pii/S036054421931268X [Accessed Nov 24, 2019].

(34) Sharma R, Subramani K. Preparation and Characterization of Surfactant Coated Ce-Zr Nanoparticles and Nanofuel. *Journal of ASTM International.* 2012; 9 104429. Available from: doi: 10.1520/JAI104429 [Accessed Nov 29, 2019].

(35) Gan Y, Qiao L. Combustion and flame. *Combustion and flame.* 1957; 158 (2): 354-368. Available from: http://www.sciencedirect.com/science/article/pii/S0010218010002488 .

(36) Shaafi T, Velraj R. Influence of alumina nanoparticles, ethanol and isopropanol blend as additive with diesel–soybean biodiesel blend fuel: Combustion, engine performance and emissions. *Renewable Energy.* 2015; 80 655-663. Available from: doi: 10.1016/j.renene.2015.02.042 Available from: http://www.sciencedirect.com/science/article/pii/S0960148115001585 [Accessed Dec 9, 2019].

(37) Jones M, Li C, Afjeh A, Peterson G. Experimental study of combustion characteristics of nanoscale metal and metal oxide additives in biofuel (ethanol). *Nanoscale Research Letters.* 2011; 6 (1): 1-12. Available from: doi: 10.1186/1556-276X-6-246 Available from: https://www.ncbi.nlm.nih.gov/pubmed/21711760 .

(38) Kumar S, Dinesha P, Bran I. Experimental investigation of the effects of nanoparticles as an additive in diesel and biodiesel fuelled engines: a review. *Biofuels.* 2019; 10 (5): 615-622. Available from: doi: 10.1080/17597269.2017.1332294 Available from: https://doi.org/10.1080/17597269.2017.1332294 [Accessed Dec 9, 2019].

(39) Arockiasamy P, Anand RB. Performance, Combustion and Emission Characteristics of a D.I. Diesel Engine Fuelled with Nanoparticle Blended Jatropha Biodiesel. *Periodica Polytechnica Mechanical Engineering.* 2015; 59 (2): 88-93. Available from: doi: 10.3311/PPme.7766 Available from: https://pp.bme.hu/me/article/view/7766 [Accessed Dec 9, 2019].

(40) Kim DM, Baek SW, Yoon J. Ignition characteristics of kerosene droplets with the addition of aluminum nanoparticles at elevated temperature and pressure. *Combustion and Flame.* 2016; 173 106-113. Available from: doi: 10.1016/j.combustflame.2016.07.033 Available from: https://www.sciencedirect.com/science/article/pii/S0010218016301973 .

(41) Hajjari M, Ardjmand M, Tabatabaei M. Experimental investigation of the effect of cerium oxide nanoparticles as a combustion-improving additive on biodiesel oxidative stability: mechanism. *RSC Advances.* 2014; 4 (28): 14352-14356. Available from: doi: 10.1039/C3RA47033D Available from: https://pubs.rsc.org/en/content/articlelanding/2014/ra/c3ra47033d [Accessed Dec 9, 2019].

(42) Sajeevan AC, Sajith V. Diesel Engine Emission Reduction Using Catalytic Nanoparticles: An Experimental Investigation. *Journal of Engineering.* 2013; 2013 e589382. Available from: doi: 10.1155/2013/589382 Available from: https://www.hindawi.com/journals/je/2013/589382/ [Accessed Dec 9, 2019].

(43) Khond VW, Kriplani VM. Effect of nanofluid additives on performances and emissions of emulsified diesel and biodiesel fueled stationary CI engine: A comprehensive review. *Renewable and Sustainable Energy Reviews.* 2016; 59 1338-1348. Available from: doi: 10.1016/j.rser.2016.01.051 Available from: http://www.sciencedirect.com/science/article/pii/S1364032116000812 [Accessed Dec 9, 2019].

(44) Arul Mozhi Selvan V, Anand RB, Udayakumar M. Effect of Cerium Oxide Nanoparticles and Carbon Nanotubes as fuel-borne additives in Diesterol blends on the performance, combustion and emission characteristics of a variable compression ratio engine. *Fuel.* 2014; 130 160-167. Available from: doi: 10.1016/j.fuel.2014.04.034 Available from: http://www.sciencedirect.com/science/article/pii/S001623611400355X [Accessed Dec 9, 2019].

(45) Soudagar MEM, Nik-Ghazali N, Kalam MA, Badruddin IA, Banapurmath NR, Yunus Khan TM, et al. The effects of graphene oxide nanoparticle additive stably dispersed in dairy scum oil biodiesel-diesel fuel blend on CI engine: performance, emission and combustion characteristics. *Fuel.* 2019; 257 116015. Available from: doi: 10.1016/j.fuel.2019.116015 Available from: http://www.sciencedirect.com/science/article/pii/S0016236119313699 [Accessed Dec 9, 2019].

(46) Zhang J, Nazarenko Y, Zhang L, Calderon L, Lee K, Garfunkel E, et al. Impacts of a Nanosized Ceria Additive on Diesel Engine Emissions of Particulate and Gaseous Pollutants. *Environmental Science & Technology.* 2013; 47 (22): 13077-13085. Available from: doi: 10.1021/es402140u Available from: https://doi.org/10.1021/es402140u [Accessed Dec 9, 2019].

(47) Farfaletti A, Astorga C, Martini G, Manfredi U, Mueller A, Rey M, et al. Effect of Water/Fuel Emulsions and a Cerium-Based Combustion Improver Additive on HD and LD Diesel Exhaust Emissions. *Environmental Science & Technology.* 2005; 39 (17): 6792-6799. Available from: doi: 10.1021/es048345v Available from: https://doi.org/10.1021/es048345v [Accessed Dec 9, 2019].

(48) Wen D. Nanofuel as a potential secondary energy carrier. *Energy & Environmental Science.* 2010; 3 (5): 591-600. Available from: doi: 10.1039/B906384F Available from: https://pubs.rsc.org/en/content/articlelanding/2010/ee/b906384f [Accessed Nov 24, 2019].

(49) Development, Office of Research &. *Health Effects Associated with Inhalation Exposure to Diesel Emission Generated with and without CeO2 Nano Fuel Additive.* Available from: https://cfpub.epa.gov/si/si_public_record_report.cfm?dirEntryId=270926&Lab=NHEERL [Accessed Dec 13, 2019].